Structural, Optical and Luminescence Properties of ZnO Thin Films Prepared by Sol-Gel Spin-Coating Method: Effect of Precursor Concentration

R. Amari[1,2**], A. Mahroug[1,2], A. Boukhari[1,2], B. Deghfel[1,2], N. Selmi[3]

[1]*Laboratory of Materials Physics and Its Applications, Department of Physics, Faculty of Sciences, University of Mohamed Boudiaf, M'sila 28000, Algeria*

[2]*Department of Physics, Faculty of Sciences, University of Mohamed Boudiaf, M'sila 28000, Algeria*

[3]*Nuclear Research Center of Birine, Ain Oussera Box 180, Algeria*

(Received 25 July 2017)

Transparent zinc oxide (ZnO) thin films are fabricated by a simple sol-gel spin-coating technique on glass substrates with different solution concentrations (0.3–1.2 M) using zinc acetate dehydrate [$Zn(CH_3COO)_2{\cdot}2H_2O$] as precursor and isopropanol and monoethanolamine (MEA) as solvent and stabilizer, respectively. The molar ratio of zinc acetate dehydrate to MEA is 1.0. X-ray diffraction, ultraviolet-visible spectroscopy and photoluminescence spectroscopy are employed to investigate the effect of solution concentration on the structural and optical properties of the ZnO thin films. The obtained results of all thin films are discussed in detail and are compared with other experimental data.

PACS: 68.55.ag, 78.66.−w, 78.55.Et DOI: 10.1088/0256-307X/35/1/016801

Recently, zinc oxide (ZnO) has been actively investigated in several applications such as solar cells,[1] gas sensors,[2] photocatalysts,[3] light-emitting diodes,[4,5] transparent electrodes,[6] owing to its remarkable properties. ZnO has direct energy band gap (3.37 eV) and large exciton binding energy (60 meV) at room temperature, and it is inexpensive, nontoxic and abundant. Nowadays, there are many methods to prepare ZnO thin films such as spray pyrolysis,[7,8] pulsed laser deposition,[9,10] molecular beam epitaxy (MBE),[11] rf magnetron sputtering,[12] metal organic chemical vapor deposition (MOCVD),[13] photo-assisted atomic layer deposition[14] and sol-gel technique.[15,16] The sol-gel technique is used in the present work for several reasons such as low-cost procedure, uniform film thickness and large deposition areas.

Many results have shown that the structural, optical and electrical properties of ZnO thin films have a strong dependence on concentration of precursor. However, there are still many differences among them. For example, Xu *et al.*[17] found that a low concentration (0.1–0.5 M) is favorable for obtaining ZnO thin films oriented on high *c*-axes having an excellent crystalline quality, which also possesses high transmittance in the visible range. Later, a sol concentration of 0.6 was suggested by Kim *et al.*[18] in their study within the range of 0.3–1.3 M, to be the optimal value for growing ZnO thin films on FTO substrates.

The main goal of this study is to investigate the effect of solution concentration, especially slightly higher ones (0.3–1.2 M), which are seldom considered, on the structural and optical properties of the ZnO thin films synthesized on glass substrates by the sol-gel spin-coating technique after adjusting its parameters of elaboration. In addition, the mechanism of the UV and visible emissions is also discussed from the viewpoint of the structural change of the ZnO thin films.

Experimentally, the sol-gel spin coating method was used to prepare ZnO thin films grown on glass substrates. Isopropanol was used as a solvent to prepare solutions by zinc acetate dehydrate [$Zn(CH_3COO)_2{\cdot}2H_2O$] and monoethanolamine (MEA) was added as a stabilizer such that the molar ratio of zinc acetate dehydrate to MEA was fixed at 1 in a 25 mL solution. The precursor concentrations were 0.3, 0.5, 0.7, 0.9 and 1.2 M. The solutions were stirred at 65℃ for 2 h to obtain clear and homogeneous solutions and then aged at room temperature for 24 h. Before the deposition process, the glass substrates were cleaned in ethanol and acetone for 10 min each by using an ultrasonic cleaner and then washed with deionized water and dried. The solution was deposited on a glass substrate at a rate of 2800 rpm for 30 s. To evaporate the solvent and remove organic residuals completely, the films were then preheated in a furnace at 250℃ for 10 min. This process (coating and preheating) was repeated 15 times. Then, the films were annealed at 500℃ for 60 min under ambient air.

The structural properties of the ZnO thin films were characterized by an x-ray diffractometer (XRD) (Bruker 8 Advance) with Cu Kα radiation (λ = 1.5406 Å). Photoluminescence (PL) measurements at room temperature were carried out using a spectrofluorimeter (Perkin Elmer LS 50B) as an excitation source at 325 nm. The optical transmission spectra were measured using an ultraviolet-visible (UV-vis) spectrophotometer (UV-3101 PC-Shimadzu) in the wavelength region of 300–800 nm.

We begin with displaying the x-ray diffraction (XRD) patterns of the ZnO thin films prepared with

**Corresponding author. Email: a.lamari28@gmail.com

© 2018 Chinese Physical Society and IOP Publishing Ltd

concentrations of 0.3–1.2 M (Fig. 1). The peaks are identified as (100), (002), (101), (102), (110), (103) and (112) reflection planes for a polycrystalline hexagonal wurtzite structure (JCPDS 75-0576).[8] It was observed that the intensity of all peaks increases with the solution concentration.

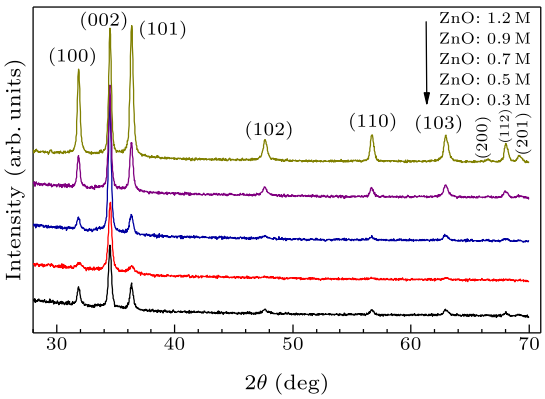

Fig. 1. XRD patterns for ZnO thin films with different sol concentrations.

In addition, the lattice parameters $a = b$ and c of the samples are calculated using

$$\sin^2(\theta) = \frac{\lambda^2}{4}\left[\frac{4}{3}\left(\frac{h^2+hk+k^2}{a^2}\right)+\frac{l^2}{c^2}\right],$$

where h, k and l are Miller's indices, θ is the diffraction angle, and λ is the incident wave-length of the Cu $K\alpha$ radiation ($\lambda = 1.5406$ Å). The values of lattice parameters are listed in Table 1. Our values are very close to the experimental ones with a relative deviation up to 0.49% for $a = b$ and 0.13% for c in the worst case.

Table 1. Lattice parameters of ZnO films deposited at various precursor concentrations. C: sol concentration.

C (M)	$a = b$ (Å)		c (Å)	
	Present	Exp.	Present	Exp.
0.3	3.250	3.254[19]	5.205	5.208[19]
0.5	3.249	3.233[20]	5.204	5.210[20]
0.7	3.247	3.261[20]	5.203	5.210[20]
0.9	3.246		5.202	
1.2	3.244		5.2006	
Bulk(JCPDS 75-0576)[8]	3.242		5.194	

Also, the preferential orientation was characterized using the texture coefficient $\mathrm{TC}_{(hkl)}$ estimated from [21–24]

$$\mathrm{TC}_{(hkl)} = \frac{I_{(hkl)}}{I_{0(hkl)}}\left[\frac{1}{N}\sum_{1}^{N}\left(\frac{I_{(hkl)}}{I_{0(hkl)}}\right)\right]^{-1},$$

where N, $I_{0(hkl)}$ are $I_{(hkl)}$ the number of diffraction peaks, the intensity of the standard powder diffraction peak and the measured relative intensity of a diffraction peak, respectively. Here $\mathrm{TC}_{(hkl)} = 1$ indicates a sample with randomly oriented crystallite, while values higher than 1 indicate the abundance of crystallites in a given (hkl) direction. Furthermore, values between 0.00 and 1.00 indicate the lack of grains orientated in the considered direction. The calculated values of $\mathrm{TC}_{(hkl)}$ for all peaks are given in Fig. 2. It can be seen that the highest $\mathrm{TC}_{(hkl)}$ value is in the (002) plane for all ZnO thin films. This does mean that all prepared films with different concentrations have a preferred growth orientation along c-axis, i.e., the (002) plane. In addition, these results indicate that the degree of c-axis orientation for the ZnO thin films depends on the sol concentration. Moreover, the highest values of TC for the main peak (002) of the ZnO thin films obtained from sol concentrations greater than 0.7 M display a tendency to decrease from 4.00 to 2.02, whereas it exhibits an upward trend when the sol concentration increases from 0.3 to 0.7 M. Consequently, the higher value of texture coefficient at 0.7 M concentration reveals a better crystallinity of thin film.

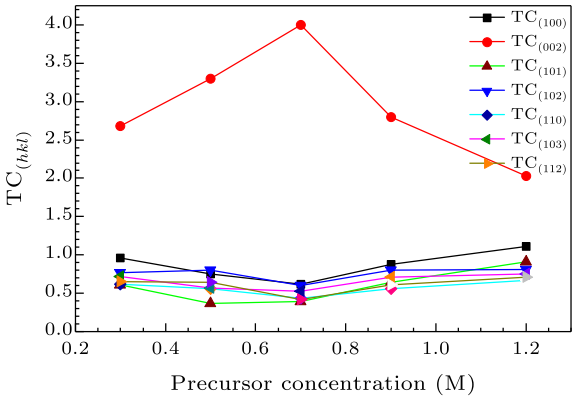

Fig. 2. Variation of texture coefficient ($\mathrm{TC}_{(hkl)}$) values of ZnO films at various sol concentrations.

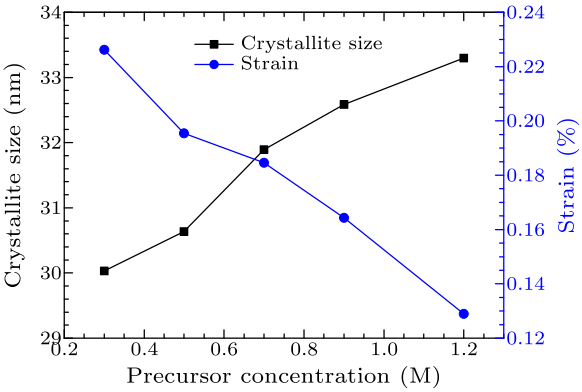

Fig. 3. Strain and crystallite size of the ZnO thin films at various sol concentrations.

The full width at half maximum (FWHM) of a given diffraction peak in the XRD pattern is used to calculate the average crystallite size of the ZnO thin films from the Debye Scherrer formula[18]

$$D = \frac{k\lambda}{\beta\cos\theta},$$

where k is a constant taken as 0.9, λ is the x-ray wavelength ($\lambda = 1.5406$ Å), β is the full width at half max-

imum (FWHM), and θ is the Bragg angle. The crystallite size of the ZnO thin films using the (002) peak is then presented in Fig. 3.

In addition, the following formula is used to calculate the strain (ε_{zz}) values,[25,26]

$$\varepsilon_{zz} = \frac{c - c_0}{c_0} \times 100\%,$$

where c and c_0 are the lattice parameters of the strained films calculated from the x-ray diffraction data and the unstrained lattice parameter of bulk ZnO,[8] respectively. The obtained values of c-axis strain are also depicted together with the crystallite size of the ZnO thin films in Fig. 3. It was observed that the crystallite size values for the ZnO thin films increases with the precursor molar concentration, which leads to the increase of the probability of more solute to be gathered together forming a grain, due to the electrostatic interaction between the solute particles.[15] Furthermore, the calculated values of the crystallite size vary slightly in the range of 30.03–33.43 nm, which are comparable with those found by Malek *et al.*[25] In contrast to the crystallite size tendency, the values of c-axis strain decrease with the increasing precursor molar concentration due to the existence of the more relaxed films.[15,25,27]

Next, we investigate the optical transmittance spectra of thin films in the wavelength range of 300–800 nm at room temperature, which are presented in Fig. 4. From Fig. 4, it can be observed that the average transmittance in the visible region is larger than 85% for most films (except for 0.9 and 1.2 M), indicating that the films are transparent in this region. Furthermore, our values of average transmittance are tabulated in Table 2 together with those of other works,[17,22,25,28–30] which are close to one another. The reported values decrease generally with the increasing ZnO sol concentrations from 0.3 M to 1.2 M. There are many factors that affect the transmittance of thin films such as film thickness, density of grain boundary and surface roughness.[17] Here the variation of the crystallite size is not appreciable (from 30 to 33.5 nm) to observe its effect on the transmittance of thin films. In addition, it is well known that the film thickness would increase with the solution concentration,[17,23,30] which may affect the scattering of light and then the transmittance. On the other hand, the transmission decreases sharply for all films near the ultraviolet region due to the band gap absorption.

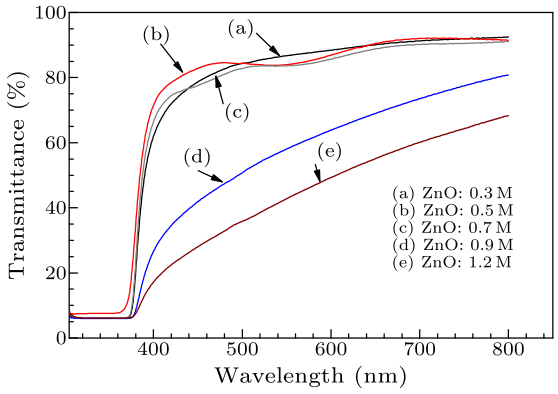

Fig. 4. Transmittance spectra of the ZnO thin film at various sol concentrations.

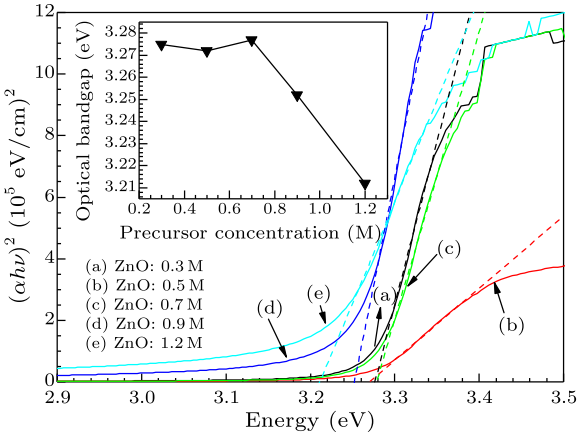

Fig. 5. Plot of $(\alpha h\nu)^2$ versus photon energy ($h\nu$). The inset shows the variation in the optical band-gap energy of ZnO film with different sol concentrations.

Table 2. Transmittance and bandgap of ZnO films deposited at various precursor concentrations.

ZnO concentration (M)	Transmittance (%)		Band gap (eV)			
	Present	Exp.	Present		Exp.	
0.3	∼ 86%	∼ 87%[28]	3.275	3.06[28]	3.288[17]	3.297[30]
0.5	∼ 86%	∼ 85%[29]	3.272	3.269[29]	3.284[17]	3.297[30]
0.7	∼ 85%	∼ 80%[28]	3.277	3.298[28]	3.279[17]	3.279[30]
0.9	∼ 61%	∼ 76%[30]	3.252			3.271[30]
1.0		∼ 75%[25]		3.266[25]	3.279[17]	3.281[22]
1.2	∼ 47%		3.212			

The absorption coefficient α is determined from the transmittance measurements using Lambert's law[18]

$$\alpha = \frac{1}{t} \ln(1/T),$$

where T is the transmittance, and t is the thickness of the film. Then, the band gap E_g is evaluated using the Tauc equation[21]

$$(\alpha h\nu)^2 = C(h\nu - E_g),$$

where α is the absorption coefficient, C is a constant, and $h\nu$ is the photon energy. Figure 5 shows $(\alpha h\nu)^2$ versus the photon energy $h\nu$. From the inset of Fig. 5,

the optical band gap is seen to vary slightly when the sol concentration is increased from 0.3 to 0.7 M, while it decreases sharply from 3.277 to 3.212 eV for precursor concentration higher than 0.7 M. This may be due to the change in the strain and the growth of the ZnO thin films along the *c*-axis. Furthermore, our results of the optical band gap (Table 2) vary within the reported values.[17,22,25,28–30]

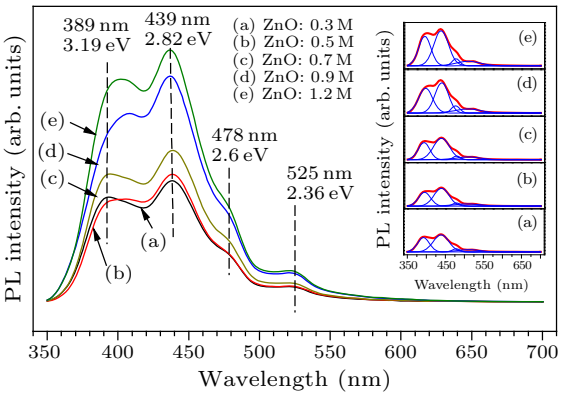

Fig. 6. PL spectra of the ZnO thin films with different sol concentrations.

Finally, we investigate the effect of the precursor concentration on the PL properties of the ZnO thin films. Figure 6 shows the PL spectra of ZnO thin films for different precursor concentrations. To analyze the contribution caused by various defects' PL spectra of the films, experimental data are fitted by multi-peak Gaussian shape. The fitting results are shown in the inset of Fig. 6. It can be seen that the PL spectra present near-band-edge (NBE) emission for all thin films, which is assigned to the recombination of free excitons.[22,30] Moreover, the intensity of the NBE emission peak increases and shifts slightly from 389 nm to 397 nm with the increasing precursor concentration. These results confirm the evolution of the band gap affected by the strain. More visible emission peaks are observed at 439 nm (2.83 eV), 478 nm (2.6 eV) and 525 nm (2.36 eV) for all thin films. Their intensities increase with the increasing solution concentration. Although the origin of these emissions has not been decisively understood,[30–32] Table 3 summarizes the visible emission peaks and their origins as reported by other researchers.[17,19,29,33–44] This may give more insights to the suggested origins of different peaks in the visible emission region. Combining these results and analyses, a schematic view of the proposed energy band diagram is presented in Fig. 7 for ZnO thin films.

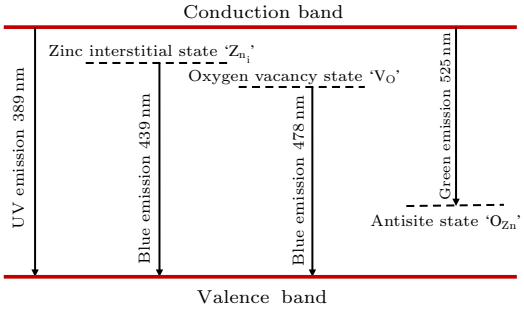

Fig. 7. Schematic view of the proposed energy band diagram.

Table 3. Visible emission peaks and their origin as reported by other researchers.

Region	Emission peak at nm (eV)	Origin	References
Blue	439 (2.82)	Electron transition from the interstitial Zn to the top of the valence band	Ref. [19]
	466 (2.66) and 472 (2.62)	Zn interstitial defects lead to the blue emission	Ref. [17]
	445 (2.79)	Oxygen vacancies V_O	Ref. [30]
	475 (2.61)	Zinc interstitial Zn_i	Ref. [30]
	468 (264)	Transition from bottom of the conduction band to oxygen related defects (oxygen vacancies or oxygen interstitials)	Ref. [34]
	486 (2.55)	The blue emission is mainly associated with Zn vacancy and Zn interstitial	Ref. [35]
	434 (2.85)	Caused by intrinsic defects and donor–acceptor pair recombination	Ref. [36]
	459 (2.7)	Electron transition from Zn_i to the V_{Zn}	Ref. [37]
	446 (2.78)	Electron transition from the shallow donor level of V_O and Zn_i to the valence band	Ref. [38]
	449 (2.76)	The formation of V_O^+ centers	Ref. [39]
	495 (2.50)	Oxygen vacancy	Ref. [44]
	521 (2.38)	Oxygen vacancies in ZnO	Ref. [19]
Green	510 (2.43)	The presence of ionized oxygen vacancies and zinc interstitial in ZnO matrix	Ref. [40]
	520 (2.38)	O_{Zn}	Ref. [44]
	521 (2.38)	Transition from conduction band to oxide antisite defects O_{Zn}	Ref. [39]
	521 (2.38)	The emission is mainly associated with Zn vacancy and Zn interstitial	Ref. [35]
	525 (2.36)	Due to the presence of singly occupied oxygen vacancy	Ref. [42]
	533 (2.32)	The oxygen vacancies-related defects	Ref. [43]
	558 (2.22)	The formation of V_O^{++} centers	Ref. [39]

It is assumed that the sharp and high intensity peak around 439 nm (2.83 eV), in blue region, may be attributed to the transition of electron from interstitial Zn_i to the valence band, and the second blue emission, around 478 nm (2.6 eV), may be originated from the electron transition from the level of the ionized oxygen vacancies to the valence band. The samples also show a green emission with a peak centered at 525 nm (2.36 eV), which has been attributed by some researchers to the transition from conduction band to the O_{Zn} level.

In summary, the structural and optical properties of ZnO thin films grown on glass substrates using the sol-gel spin-coating method have been found to be influenced by the precursor concentrations. The obtained results show that all samples have a polycrystalline hexagonal wurtzite structure and are preferentially oriented along the (002). Moreover, the higher values of texture coefficient at 0.7 M concentration reveal a high crystallinity of the thin film. The optical band gap varies slightly when the sol concentration is increased from 0.3 to 0.7 M, while it decreases monotonously for precursor concentration higher than 0.7 M. In addition, the transmission spectra exhibit a high transparency in the visible region at sol concentrations below 0.7 M. A UV emission is observed, which might be originated from exciton recombination. The samples also show three visible emissions that could be due to defect emission in ZnO films.

References

[1] Bhosle V, Prater J T, Yang F, Burk D, Forrest S R and Narayan J 2007 *J. Appl. Phys.* **102** 023501
[2] Shishiyanu S T, Shishiyanu T S and Lupan O I 2005 *Sens. Actuators* B **107** 379
[3] Maeda K, Takata T, Hara M, Saito N, Inoue Y, Kobayashi H and Domen K 2005 *J. Am. Chem. Soc.* **127** 8286
[4] Cao H T, Sun C, Pei Z L, Wang Y and Wen L S 2004 *J. Mater. Sci.: Mater. Electron.* **15** 169
[5] Kim H, Horwitz J S, Kim W H, Mäkinen A J, Kafafi Z H and Chrisey D B 2002 *Thin Solid Films* **420–421** 539
[6] Choi K, Kim J, Lee Y and Kim H 1999 *Thin Solid Films* **341** 152
[7] Gaikwad R S, Jagdale S B and Pol P B 2014 *Asian J. Multidiscip. Stud.* **2** 109
[8] Prasada Rao T and Santhoshkumar M C 2009 *Appl. Surf. Sci.* **255** 4579
[9] Günster J, Görke R, Heinrich J G and Souda R 2001 *Appl. Surf. Sci.* **173** 76
[10] Vishnoi S, Kumar R and Singh B P 2014 *J. Intense Pulsed Lasers Appl. Adv. Phys.* **4** 35
[11] Kato H, Sano M, Miyamoto K and Yao T 2003 *Jpn. J. Appl. Phys.* **42** L1002
[12] Menon R, Sreenivas K and Gupta V 2008 *J. Appl. Phys.* **103** 094903
[13] Pagni O, James G R and Leitch A W R 2004 *Phys. Status Solidi* C **1** 864
[14] Yamamoto Y, Saito K, Takahashi K and Konagai M 2001 *Sol. Energy Mater. Sol. Cells* **65** 125
[15] Dutta M, Mridha S and Basak D 2008 *Appl. Surf. Sci.* **254** 2743
[16] Caglar Y, Caglar M and Ilican S 2012 *Curr. Appl. Phys.* **12** 963
[17] Xu L, Zheng G, Miao J and Xian F 2012 *Appl. Surf. Sci.* **258** 7760
[18] Kim Y and Leem J Y 2016 *J. Nanosci. Nanotechnol.* **16** 5186
[19] Baneto M, Enesca A, Lare Y, Jondo K, Napo K and Duta A 2014 *Ceram. Int.* **40** 8397
[20] Tazerout M, Chelouche A, Touam T, Djouadi D, Boudjouan F, Khodja S, Ouhenia S, Fischer A and Boudrioua A 2014 *Eur. Phys. J. Appl. Phys.* **67** 10502
[21] Mahroug A, Boudjadar S, Hamrit S and Guerbous L 2014 *J. Mater. Sci.: Mater. Electron.* **25** 4967
[22] Kim I, Kim Y, Nam G, Kim D, Park M, Kim H, Lee W and Leem J Y 2014 *J. Korean Phys. Soc.* **65** 480
[23] Saleem M M, Fang L, Ruan H B, Wu F, Huang Q L, Xu C L and Kong C Y 2012 *Int. J. Phys. Sci.* **7** 2971
[24] Lupan O, Chowb L, Shishiyanu S, Monaicoc E, Shishiyanu T, Sontea V, Roldan Cueny B, Naitabdi A, Park S and Schulte A 2009 *Mater. Res. Bull.* **44** 63
[25] Malek M F, Mamat M H, Sahdan M Z, Zahidi M M, Khusaimi Z and Mahmood M R 2013 *Thin Solid Films* **527** 102
[26] Raoufi D and Raoufi T 2009 *Appl. Surf. Sci.* **255** 5812
[27] Mridha S and Basak D 2007 *Mater. Res. Bull.* **42** 875
[28] Brien S O, K Koh L H and Crean G M 2008 *Thin Solid Films* **516** 1391
[29] Nagayasamy N, Gandhimathination S and Veerasamy V 2013 *Open J. Metal* **3** 8
[30] Liu J, Zhao X, Duan L, Cao M, Guan M and Guo W 2013 *J. Mater. Sci.: Mater. Electron.* **24** 4932
[31] Lee G H, Yamamoto Y, Kourogi M and Ohtsu M 2001 *Thin Solid Films* **386** 117
[32] Cheng T X W, Wu P and Zou X 2006 *J. Appl. Phys.* **100** 54311
[33] Zeng W P C B, Duan G T, Li Y, Yang S K and Xu X X 2010 *Adv. Funct. Mater.* **20** 561
[34] Gayen R N, Sarkar K, Hussain S, Bhar R and Pal K 2011 *Indian J. Pure Appl. Phys.* **49** 470
[35] Li Y, Xu L, Li X, Shen X and Wang A 2010 *Appl. Surf. Sci.* **256** 4543
[36] Chand P, Gaur A, Kumar A and Kumar U 2014 *Ceram. Int.* **40** 11915
[37] Zhang Q P W D H and Xue Z Y 2002 *J. Phys.* D **35** 2837
[38] Wei X Q, Man B Y, Liu M, Xue C S, Zhuang H Z and Yang C 2007 *Physica* B **388** 145
[39] Karthikeyan B and Pandiyarajan T 2010 *J. Lumin.* **130** 2317
[40] Petersen J, Brimont, Gallart M, Cregut O, Schmerber G, Gilliot P, Honerlage B, Bouillet C U, Rehspringer J L, Leuvrey C, Colis S, Slaoui A and Dinia A 2009 *Microelectron. J.* **40** 239
[41] Sagar P, Shishodia P K, Mehra R M, Okada H, Wakahara A and Yoshida A 2007 *J. Lumin.* **126** 800
[42] Karmakar R, K Neogi S, Banerjee A and Bandyopadhyay S 2012 *Appl. Surf. Sci.* **263** 671
[43] Liu Y, Zhang H, An X, Gao C, Zhang Z and Zhou J 2010 *J. Alloys Compd.* **506** 772
[44] Djurisic A B, Ng A M C and Chen X Y 2010 *Prog. Quantum Electron.* **34** 191